Fish Locomotion: Recent Advances and New Directions

George V. Lauder

Museum of Comparative Zoology, Harvard University, Cambridge, Massachusetts 02138; email: glauder@oeb.harvard.edu

Annu. Rev. Mar. Sci. 2015. 7:521–45

First published online as a Review in Advance on September 19, 2014

The *Annual Review of Marine Science* is online at marine.annualreviews.org

This article's doi: 10.1146/annurev-marine-010814-015614

Keywords

swimming, kinematics, hydrodynamics, robotics

Abstract

Research on fish locomotion has expanded greatly in recent years as new approaches have been brought to bear on a classical field of study. Detailed analyses of patterns of body and fin motion and the effects of these movements on water flow patterns have helped scientists understand the causes and effects of hydrodynamic patterns produced by swimming fish. Recent developments include the study of the center-of-mass motion of swimming fish and the use of volumetric imaging systems that allow three-dimensional instantaneous snapshots of wake flow patterns. The large numbers of swimming fish in the oceans and the vorticity present in fin and body wakes support the hypothesis that fish contribute significantly to the mixing of ocean waters. New developments in fish robotics have enhanced understanding of the physical principles underlying aquatic propulsion and allowed intriguing biological features, such as the structure of shark skin, to be studied in detail.

INTRODUCTION

Analysis of the mechanics of fish swimming has a long history, dating generally to the time of Aristotle and in a more detailed form to early work by Borelli (1680; Alexander 1983 provides a good overview of the history of research on fish locomotion). Since this early work, continued interest in understanding how aquatic animals such as fish generate propulsive forces to swim and maneuver has been motivated at least in part by curiosity about the many intriguing structural and functional adaptations that fish have for locomotion, and also by interest in understanding the complex mechanics of moving through a relatively dense and viscous fluid such as water. Many useful review papers and books provide an overview of fish locomotion, beginning with the classic works of Sir James Gray (1953, 1968), Neill Alexander (1967), and Paul Webb (1975) and continuing to more recent overview volumes (Blake 1983, Domenici & Kapoor 2010, Lighthill 1975, Maddock et al. 1994, Shadwick & Lauder 2006, Videler 1993, Webb & Weihs 1983, Wu et al. 1975) and review papers (e.g., Drucker et al. 2006; Fish & Lauder 2006, 2013; Lauder 2006; Lauder & Tytell 2006; Liao 2007; Maia et al. 2012; Shadwick & Goldbogen 2012; Triantafyllou et al. 2000; Wardle et al. 1995; Webb & Blake 1985). In this review, I do not recapitulate results previously summarized in those publications or present an updated overview of what is now a very diverse topic. Rather, my goal is to focus on selected new approaches and techniques for understanding how fish move through the water and to put these recent results into the context of classical studies of fish swimming.

Recent developments in the study of fish locomotion include analysis of the motion of the center of mass (COM), an active topic of investigation in studies of terrestrial locomotion but nearly totally neglected in experimental studies of swimming fish. In addition, new approaches to imaging water flows in three dimensions (3D) and calculating forces on swimming bodies have allowed a better understanding of the momentum shed into the wake by fish movements, and studies have now shown that the cumulative effect of fish wake flows contributes significantly to the mixing of ocean waters. Finally, new developments in fish robotics have enhanced understanding of the physical principles underlying aquatic propulsion and allowed intriguing biological features, such as the structure of shark skin, to be studied in detail. Robotic models of fish, varying from simple two-dimensional (2D) approaches to complex engineered biomimetic models, offer considerable promise as a new approach to understanding the structural and functional diversity of fish.

THE DIVERSITY OF FISH SWIMMING PATTERNS

Fish locomotion involves the deformation of the body and fins. Understanding changes in fin and body shape in 3D is critical to linking structural deformations to patterns of fluid flow and to developing accurate computational fluid dynamic models of swimming fish (Borazjani & Sotiropoulos 2009, Borazjani et al. 2012, Bozkurttas et al. 2009, Dong et al. 2010, Kern & Koumoutsakos 2006). Although reviews of fish swimming often characterize the diversity of swimming patterns by the number of waves on the body and promote a complex taxon-based naming scheme (e.g., anguilliform, carangiform, and balistiform) to describe different modes of locomotion (e.g., Sfakiotakis et al. 1999), such classifications are subject to numerous exceptions and are based on a highly simplified 2D view of fish swimming.

Fish that swim using body undulations generate a wave of bending that passes from head to tail, deforming the body into a wave-like shape (**Figure 1**). The movement of this wave imparts momentum to the water in the form of increased water velocity in the immediate wake behind the fish. Although patterns of body bending can vary in the number of waves, in the form of the amplitude change of the wave along the body, and in the wave speed, the general form of the body

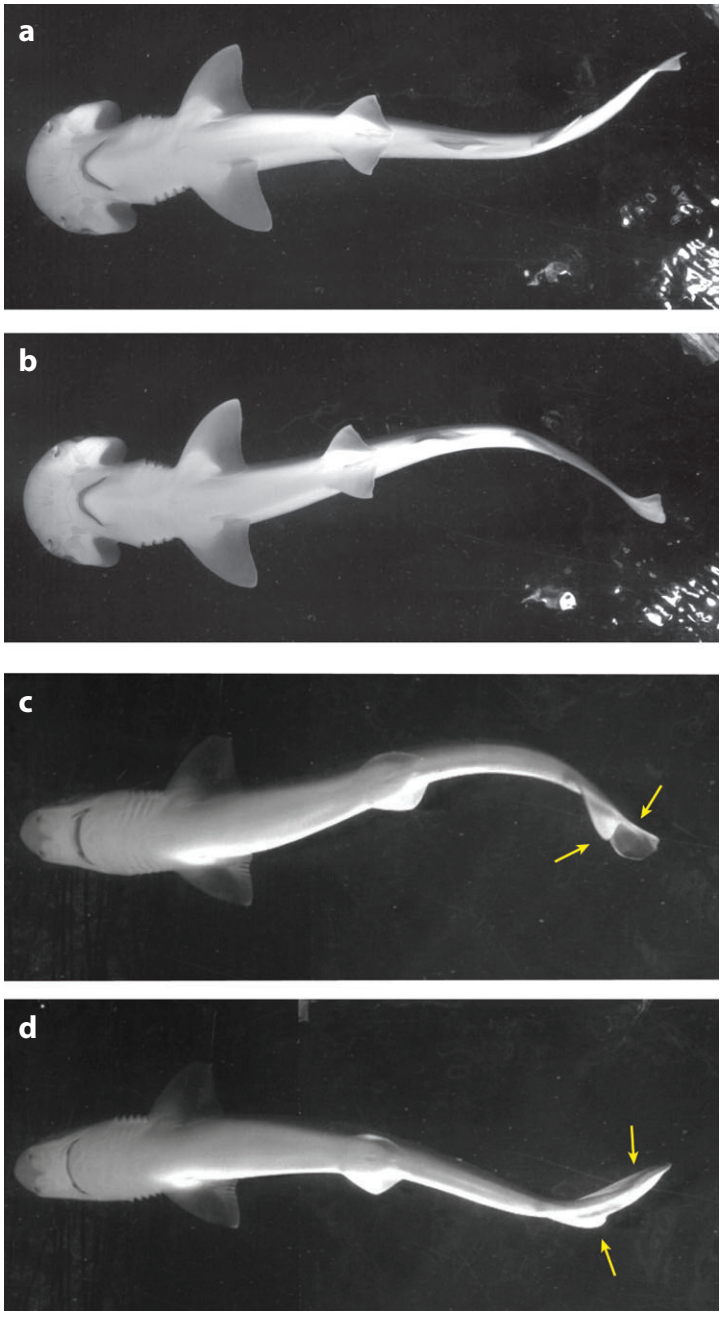

Figure 1

Pattern of undulatory body motion in swimming sharks. (*a*,*b*) A bonnethead shark (*Sphyrna tiburo*), showing the body conformation at two points when the tail is approximately 180° out of phase during a single tail beat cycle. (*c*,*d*) A spiny dogfish shark (*Squalus acanthias*) at similar points in the tail beat cycle. Note the undulatory wave on the body and the change in shape of the heterocercal (asymmetrical) tail during swimming (*arrows*).

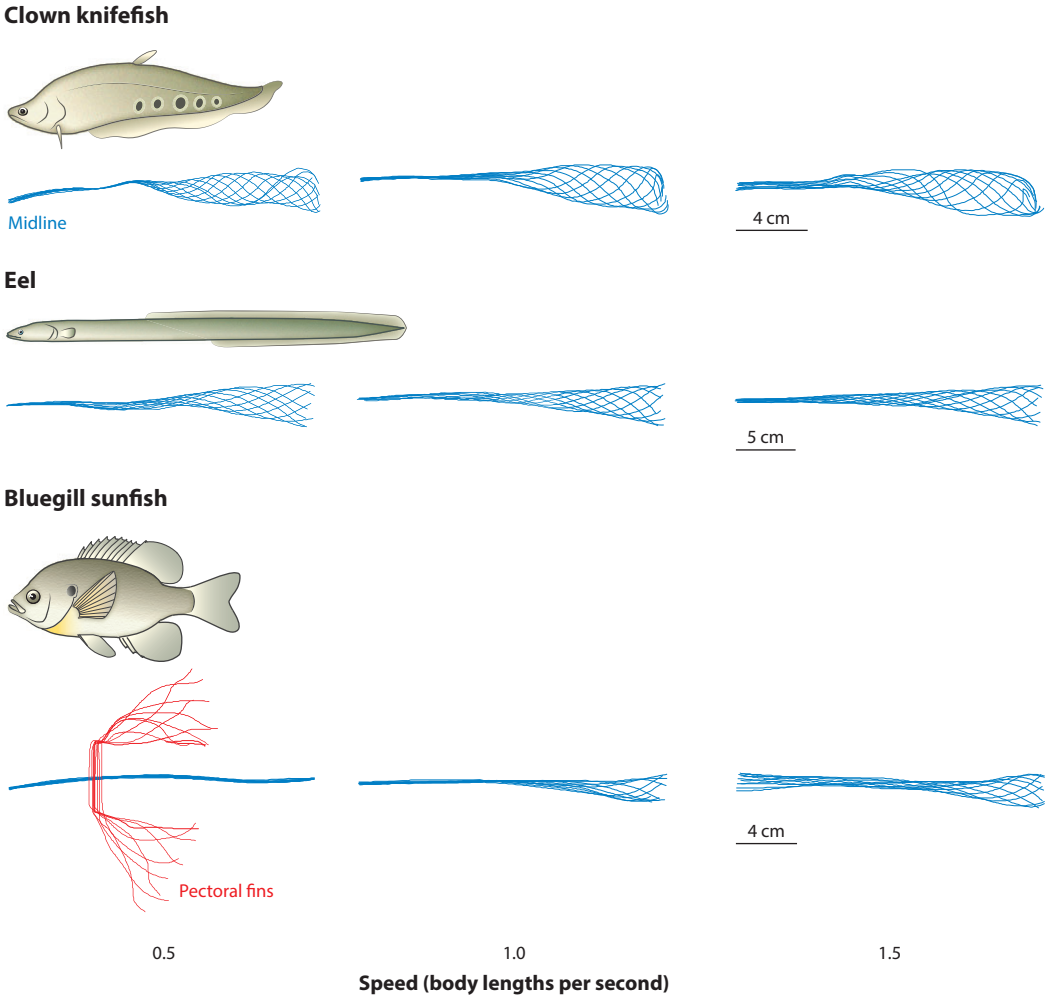

Figure 2

Representative midlines of three fish species—clown knifefish (*Notopterus chitala*), American eel (*Anguilla rostrata*), and bluegill sunfish (*Lepomis macrochirus*)—swimming at three different speeds (*blue outlines*), showing the body motions over one tail beat cycle. At their slowest swimming speed, bluegill sunfish use only their pectoral fins (*red outlines*) and hold their bodies still; body undulation begins at approximately 1 body length per second in this species. The amplitude of the tail beat does not increase significantly with increasing speed for any of the three species, and in general, fish swimming tends to be frequency modulated as speed increases. Figure adapted from Xiong & Lauder (2014).

wave is very similar among a diversity of fishes (Lauder & Tytell 2006). **Figure 2** shows the body waveforms from three species to illustrate this overall similarity, which also extends to relatively stiff fish like tuna and flexible eel-like swimmers (Donley & Dickson 2000; Donley & Shadwick 2003; Gillis 1996, 1997). Several species also exhibit gait changes, swimming with paired fins only at slow speeds and adding additional thrust-producing surfaces, such as the body and median fins, as the speed increases (Drucker 1996, Drucker & Jensen 1996, Drucker & Lauder 2000, Gibb et al. 1994, Hale et al. 2006) (bluegill sunfish in **Figure 2**).

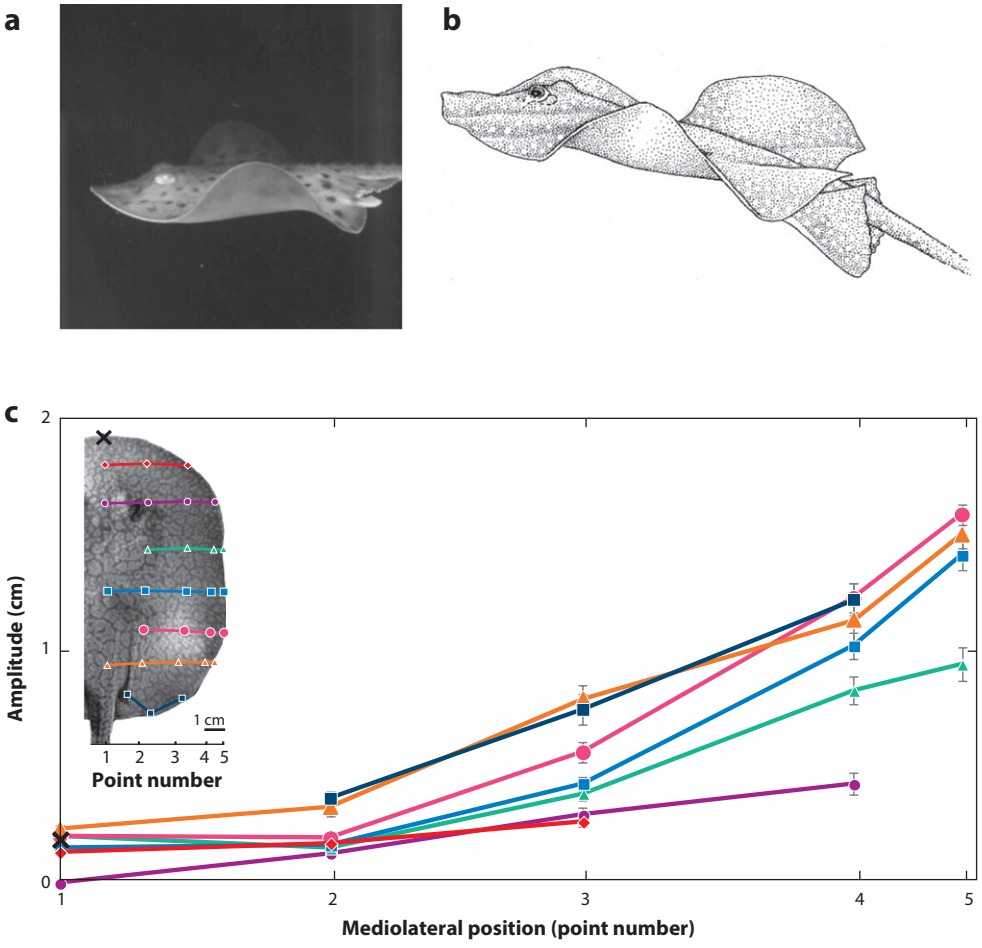

Figure 3

Locomotion in skates and stingrays. (*a*) An image from a high-speed video sequence of a little skate (*Leucoraja erinacea*). Note the large wing amplitude and the wave-like motion on the wing. (*b*) A drawing of the motion of the pectoral fin wing of a freshwater stingray (*Potamotrygon orbignyi*) during swimming. Freshwater stingrays often exhibit an inclined body posture to generate lift when swimming steadily and maintaining vertical position. (*c*) Amplitude variation along the span of the wing at the positions indicated on the stingray image (*inset*). The lateral half of the wing exhibits the majority of vertical oscillation. Error bars represent ± 1 standard error of the mean; some are obscured by symbols. Panel *a* provided by V. DiSanto, E.L. Blevins & G.V. Lauder (unpublished photograph); panels *b* and *c* adapted from Blevins & Lauder (2012).

In many species, pectoral fin locomotion can occur over the entire range of swimming speeds (Walker & Westneat 1997, Westneat 1996), and many species use paired pectoral fins as a primary locomotor structure. Batoid fishes (skates and rays) are noted for their graceful locomotion using expanded pectoral fins (**Figure 3**), and 3D deformations of these fins produce lift and thrust forces (Blevins & Lauder 2012, Macesic et al. 2013, Rosenberger 2001, Rosenberger & Westneat 1999). The pectoral fin "wing" is thrown into a complex wave-like motion that increases in amplitude from the midline toward the lateral margin and from the anterior to the posterior (**Figure 3**).

In some cases, the fin margin can curl so that the outer edge is cupped ventrally when the wing moves in the downstroke (Blevins & Lauder 2012).

Locomotion using body undulations (**Figures 1** and **2**) often involves the simultaneous and active use of additional fins, especially median fins like the dorsal and anal fins (Drucker & Lauder 2005; Maia & Wilga 2013a,b; Standen & Lauder 2005, 2007). The motion of these fins may generate additional thrust and may also be used to balance roll and yaw torques generated during locomotion.

Fish may exhibit a variety of other interesting locomotor behaviors that involve rapid linear accelerations (very poorly studied, but see Tytell 2004), escape responses (very well studied; see, e.g., Domenici & Blake 1997, Eaton & DiDomenico 1986, Eaton et al. 1977, Hale et al. 2002, Tytell & Lauder 2008, Westneat et al. 1998), and locomotion in turbulent flow patterns, which can elicit novel kinematics as the fish body interacts with larger-scale vortices shed by obstacles (Liao 2007; Liao et al. 2003a,b). Although technically not a mode of swimming, the locomotor interactions of fish with substrates are a common feature of behavioral diversity in many groups, including freshwater darters, which commonly live on stream bottoms and inhabit the boundary-layer flow region (Carlson & Lauder 2010, 2011); flatfishes (Brainerd et al. 1997, Gerstner & Webb 1998); sculpins (Webb et al. 1996); cod (Gerstner 1998); and sharks and rays (Wilga & Lauder 2001, Wilga et al. 2012).

HOW FISH SWIM

In brief, fish swim by transferring momentum to the water. But there are, of course, many details of how this is accomplished in any individual fish, and fish species differ greatly in the mechanisms of momentum transfer owing in part to the diversity of body and fin shape, fin placement and flexibility, and muscle distribution patterns in different species. Here, I discuss some new approaches to studying the kinematics, hydrodynamics, and energetics of fish propulsion.

Kinematics

Although there have been many detailed studies of fish kinematics, beginning with the pioneering descriptions by Sir James Gray (1933a–c) and continuing to the present day (selected citations from a large literature include Donley & Dickson 2000, Donley & Shadwick 2003, Gillis 1996, Hess & Videler 1984, Jagnandan & Sanford 2013, Müller et al. 2002, Ruiz-Torres et al. 2013, Shadwick & Gemballa 2006, Wardle et al. 1995, Webb 1975, Webb & Keyes 1982, Webb et al. 1984, and Youngerman et al. 2014), there is one area in which analyses of aquatic propulsion are significantly lacking: study of how the COM of swimming fish moves. Studies of terrestrial locomotion frequently focus on the COM because its motion provides critical information on locomotor dynamics (the balance of forces on a moving body) and can be used to calculate energy expenditure and efficiency. Although terrestrial analyses of COM motion focus most often on vertical excursions, the COM motion of fish swimming in the water involves significant (although small) excursions in all three dimensions (at least for some gaits), all of which could have significant implications for our understanding of the energetics and biomechanics of aquatic propulsion. Many fish species oscillate vertically when swimming with pectoral fins in a flapping motion, although some fin motion patterns may act to minimize vertical body oscillation. In addition, one might predict that minimizing horizontal COM oscillation in both the forward and sideways directions could also be energetically advantageous, but few data exist on how swimming styles impact COM motions. Surprisingly little is known about COM motion during undulatory locomotion in fish or about how COM motion might change with swimming speed and fish body shape. This is certainly

one area in which studies of fish locomotion lag substantially behind analyses of animal flight or terrestrial movement, and in this review I wish to emphasize the value of additional research in this area. Thus, rather than recapitulate previous reviews of fish body bending patterns, I focus here on the motion of the COM in undulatory fish propulsion and the relationship of COM motion to body shape and swimming style.

Figure 4 shows data on COM motion from three fish species that differ in body shape (Xiong & Lauder 2014). Tracking the pattern of body movement over the COM region in 3D in each species allowed calculation of the COM motion in the surge (forward-backward), sway (side-to-side), and heave (vertically or up-down) directions. The surge COM displacement and acceleration, reflecting the balance of thrust and drag, oscillated at twice the tail beat frequency in fish such as eels and bluegill sunfish, whereas the sway COM displacement and acceleration in these species occurred at the tail beat frequency. COM oscillations in the surge direction were on the order of 0.5–1.5 mm, or approximately 0.5% of body length, and did not change significantly with increasing swimming speed (**Figure 4**). However, sway oscillations did increase as swimming speed increased.

In this study, the COM oscillation patterns of fish with different body shapes did not correspond as one might expect, suggesting that this is an interesting area for future work. For example, the sway amplitudes of laterally compressed fish like bluegill sunfish increased with faster swimming speeds, whereas those in elongate-bodied eels did not (**Figure 4**), despite the notion that lateral flattening in fish might function to reduce side-to-side body movement and increase locomotor efficiency. The implications of fish COM motion for swimming energetics and body shape evolution are completely unexplored, and this represents one of the most interesting future areas of research in fish swimming kinematics.

Of course, most species of fish also use their fins during locomotion, and both medial (dorsal and anal) and paired (pectoral and pelvic) fins can play a key role in balancing torques and generating thrust (e.g., Standen 2008; Standen & Lauder 2005, 2007). The deformation of both median and paired fins can be considerable, and focused studies of fin flexibility and conformational change during swimming have shown that fish actively modulate their fin area and shape to vector forces for both propulsion and maneuvering and that both movement patterns and the surface area of fins can change as fish alter their swimming speed (Lauder et al. 2006). Fish tail shape in most species is also modulated throughout each swimming cycle. For example, the asymmetrical tails of sharks (**Figure 1*c,d***) undergo complex surface changes during swimming (Ferry & Lauder 1996, Wilga & Lauder 2002), and even the externally symmetrical tails of teleost fish such as the bluegill sunfish undergo substantial changes in surface area and shape. Studying 3D changes in the shapes of fish fins during swimming is technically challenging but critical to advancing our understanding of propulsion (Lauder & Madden 2006, Tytell et al. 2008).

Conformational changes in fish fins during locomotion are accomplished by an intrinsic fin musculature that is independent of the substantially more massive body musculature that powers undulatory locomotion. In addition, the fins of ray-finned fishes are supported by remarkable segmented fin rays that, as a result of their mechanical design, are able to actively resist fluid loading (**Figure 5**). The fin rays of ray-finned fishes (Actinopterygii) possess a bilaminar structure that allows the musculature attaching to the base of each half ray (hemitrich) to cause differential sliding of the ray halves, effecting the curvature of the ray as a whole (Alben et al. 2007, Flammang et al. 2013, Lauder et al. 2011b, Taft & Taft 2012). This allows segmented fin rays to be actively bent into oncoming flows and to resist fluid loading on the fin. Sharks and rays do not possess this type of fin ray, and the curvature of fin rays in these groups cannot be actively modulated.

One important role of flexible fins, not widely appreciated until recently, is to help fish sense their surroundings. In particular, fish use their pectoral fins to navigate obstacle-filled

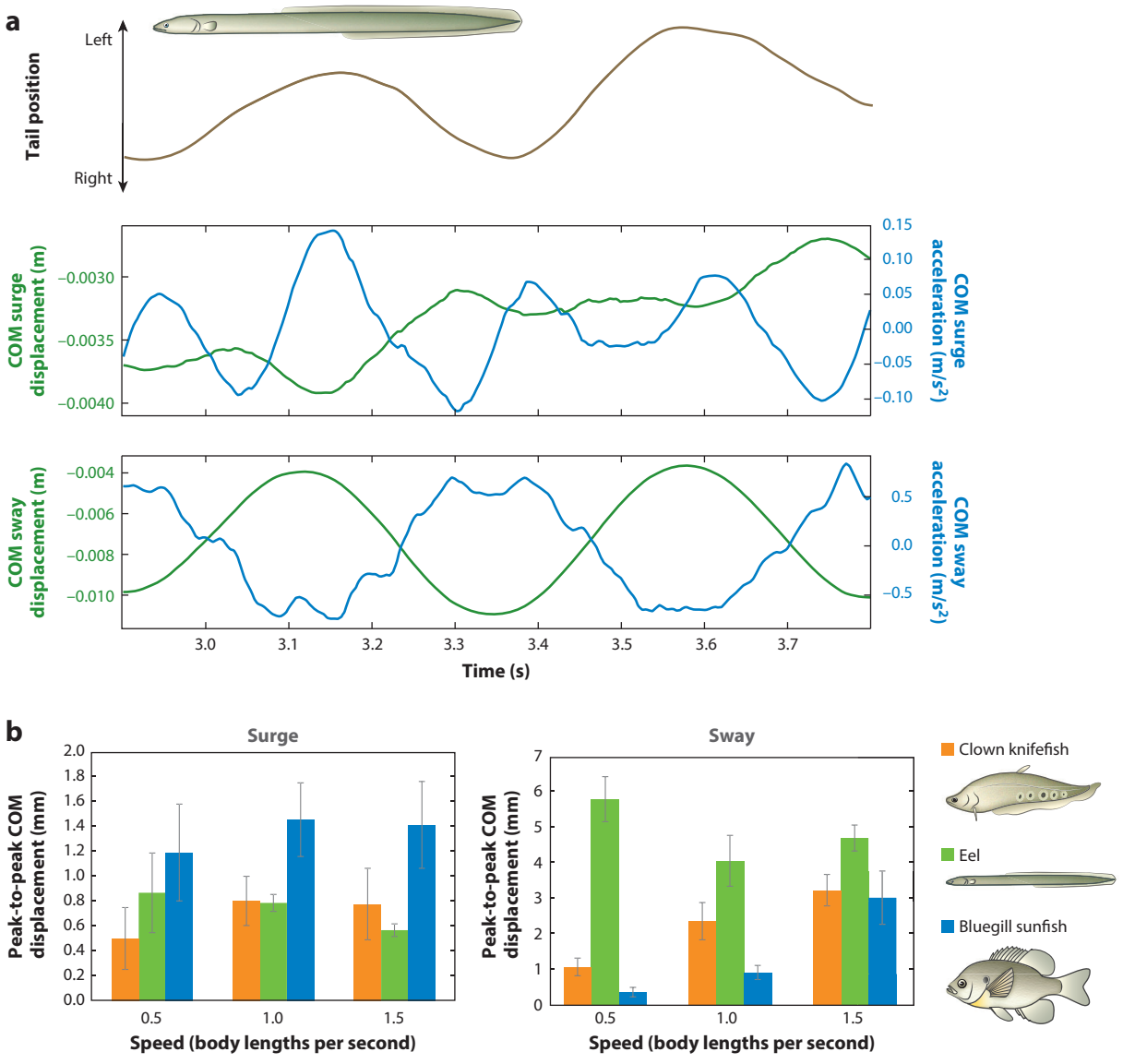

Figure 4

(*a*) The locomotor pattern of the center of mass (COM) in swimming eels (*Anguilla rostrata*) along with COM displacement and acceleration relative to tail position during locomotion at 1.5 body lengths per second. Surge (forward-backward) displacement shows a double-peak oscillation that is not evident in the sway (side-to-side) COM oscillation. Surge COM oscillation occurs at twice the tail beat frequency. (*b*) COM oscillation peak-to-peak magnitudes (i.e., double the wave amplitude) for surge and sway COM motions in three fish species at three speeds. Error bars represent ± 1 standard error of the mean. Statistical analysis (Xiong & Lauder 2014) showed a significant species effect in the surge data, whereas the sway data had significant species, speed, and species-speed interaction effects. Data from Xiong & Lauder (2014).

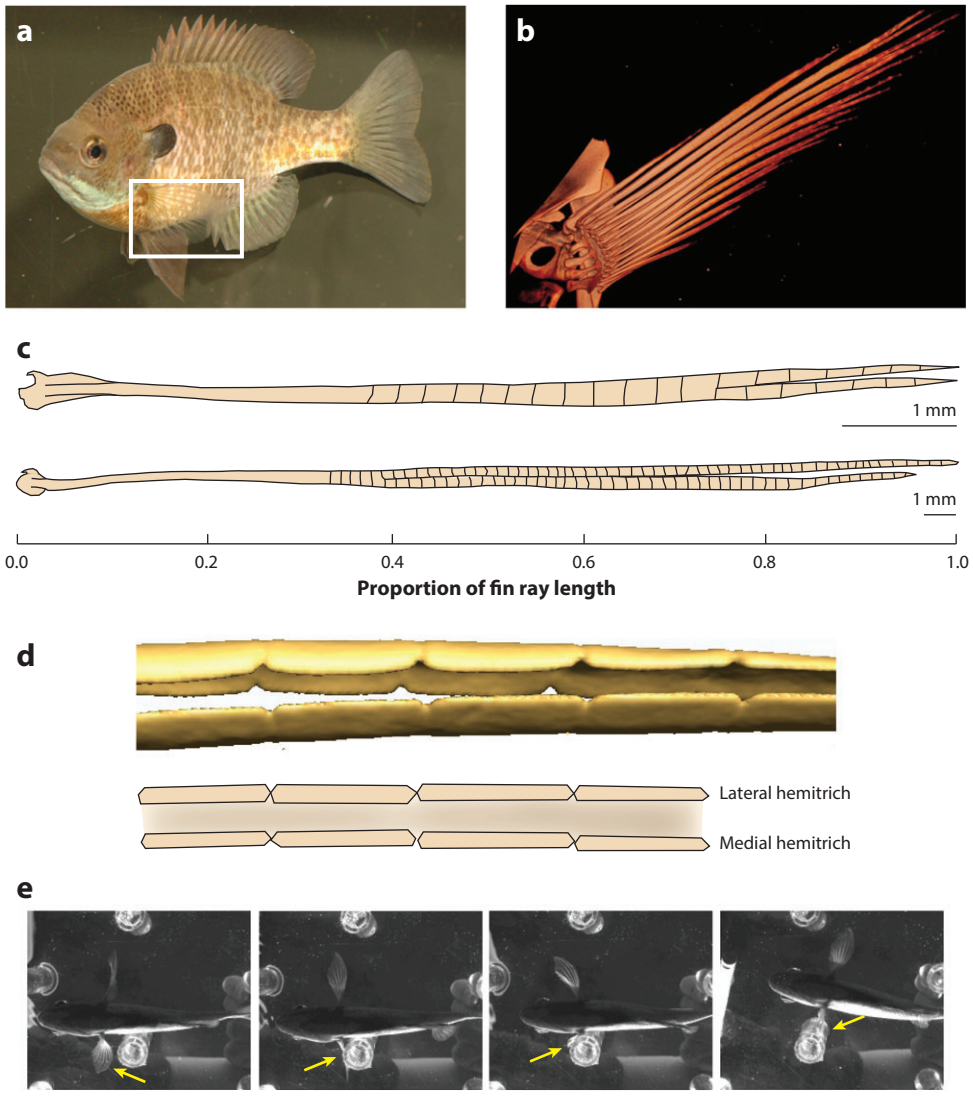

Figure 5

Fin ray structure in ray-finned fishes. (*a*) A hovering bluegill sunfish (*Lepomis macrochirus*) with extended pectoral fin (*white box*). (*b*) A computed microtomography (μCT) scan of the left pectoral fin and girdle of a bluegill sunfish. (*c*) A tracing of the longest (third) left pectoral fin ray from two bluegill sunfish, one with a total length of 6.1 cm (*top*) and one with a total length of 16.9 cm (*bottom*). (*d*) A zoomed-in view of segments from the μCT scan shown in panel *b* (*top*) and a tracing of a longitudinal section through the third fin ray of the 16.9-cm specimen shown in panel *c* (*bottom*), showing four serial segments in a ventral view. Shading represents collagen and elastic fibers connecting the lateral and medial halves of the fin ray (hemitrichs). (*e*) Video frames from a bluegill sunfish traversing an obstacle course. The pectoral fins often contact obstacles (*arrows*) and may have a sensory as well as a locomotor function. Panels *a–d* adapted from Flammang et al. (2013); panel *e* adapted from Flammang & Lauder (2013).

environments, and as these fins make contact with obstacles, they likely provide sensory information on the position and size of environmental features (Ellerby & Gerry 2011, Flammang & Lauder 2013, Williams et al. 2013, Windsor et al. 2010) (**Figure 5*e***).

Hydrodynamics

The study of the hydrodynamics of aquatic animal locomotion has been revolutionized in recent years by the technique of particle image velocimetry, which allows the visualization of water flow in the wake and around the bodies of swimming fish (selected citations from a large literature include Anderson et al. 2001; Drucker & Lauder 1999, 2002; Lauder & Madden 2008; Lauder & Tytell 2006; Müller et al. 2008; Nauen & Lauder 2002; Standen 2010; Tytell 2006; Tytell & Lauder 2004; Wilga & Lauder 2000; Windsor et al. 2008; and Wu et al. 2007). In this method, laser light is focused into a 2D light sheet, and images are then obtained from high-speed videos of particles (usually added to the water in considerable numbers) moving with the flow. Analysis of particle motion produces a velocity vector field for each pair of video frames, and using high-speed video allows a detailed time-dependent description of water flow patterns, calculation of wake vorticity, and estimation of locomotor force (e.g., Lauder & Drucker 2002, Peng et al. 2007).

The traditional 2D particle image velocimetry approach has recently been extended to volumetric (3D) imaging capability, which provides instantaneous 3D flow reconstructions of the wakes of fish bodies and fins during swimming. A 2D flow visualization provides detailed data on flow within a given plane, but multiple 2D planes of analysis must be combined to reconstruct 3D flow patterns. Using three cameras focused simultaneously into a volume within a recirculating flow tank, Flammang et al. (2011a) were able to reconstruct instantaneous volumetric flow patterns in the wake of teleost fish with symmetrical tail shapes (**Figure 6**). These volumetric images revealed the 3D structure of the linked-chain pattern of vortex rings shed by the tail and also the strong wake flows shed by the dorsal and anal fins, which interact with tail (caudal) fin flows.

A similar volumetric imaging approach to study the hydrodynamic function of the morphologically asymmetrical tails of sharks revealed a complex dual linked-ring vortex wake shed by the tail during swimming (**Figure 7**). A simple mechanical model of the angled trailing edge of the shark tail reproduced some of the wake vortex features created by sharks, showing that some of this complex structure is due solely to the angle that the trailing edge makes with the body axis. However, other features of the shark tail wake were not generated by this simple mechanical model (**Figure 7**). These data suggest that active control of the shark tail by intrinsic musculature may be responsible for the observed wake flow patterns, but exactly how the shark wake is produced by tail deformation during swimming remains unknown.

Another new area of research in fish hydrodynamics deals with the surface structure of fish and the effects of skin microstructure on swimming performance. Fish are covered with a remarkable diversity of surface ornamentation, ranging from bony scales in ray-finned fishes (Bruet et al. 2008, Goodrich 1930, Zhu et al. 2012) to the complex bony denticles on the skin of sharks (Castro 2011, Motta et al. 2012, Oeffner & Lauder 2012). Analysis of the hydrodynamic function of fish surface structures is in its infancy, in part because studying how fish surface ornamentation functions during locomotion is challenging.

Figure 8 shows skin denticles (scales) on the skin of a bonnethead shark along with the process of manufacturing a 3D biomimetic shark skin surface for hydrodynamic testing. Although there is considerable diversity in shark skin denticle structures, the denticles of many pelagic shark species commonly exhibit three surface ridges and an overhanging shape so that adjacent denticles overlap their neighbors. Typical denticles are 150–300 μm in size.

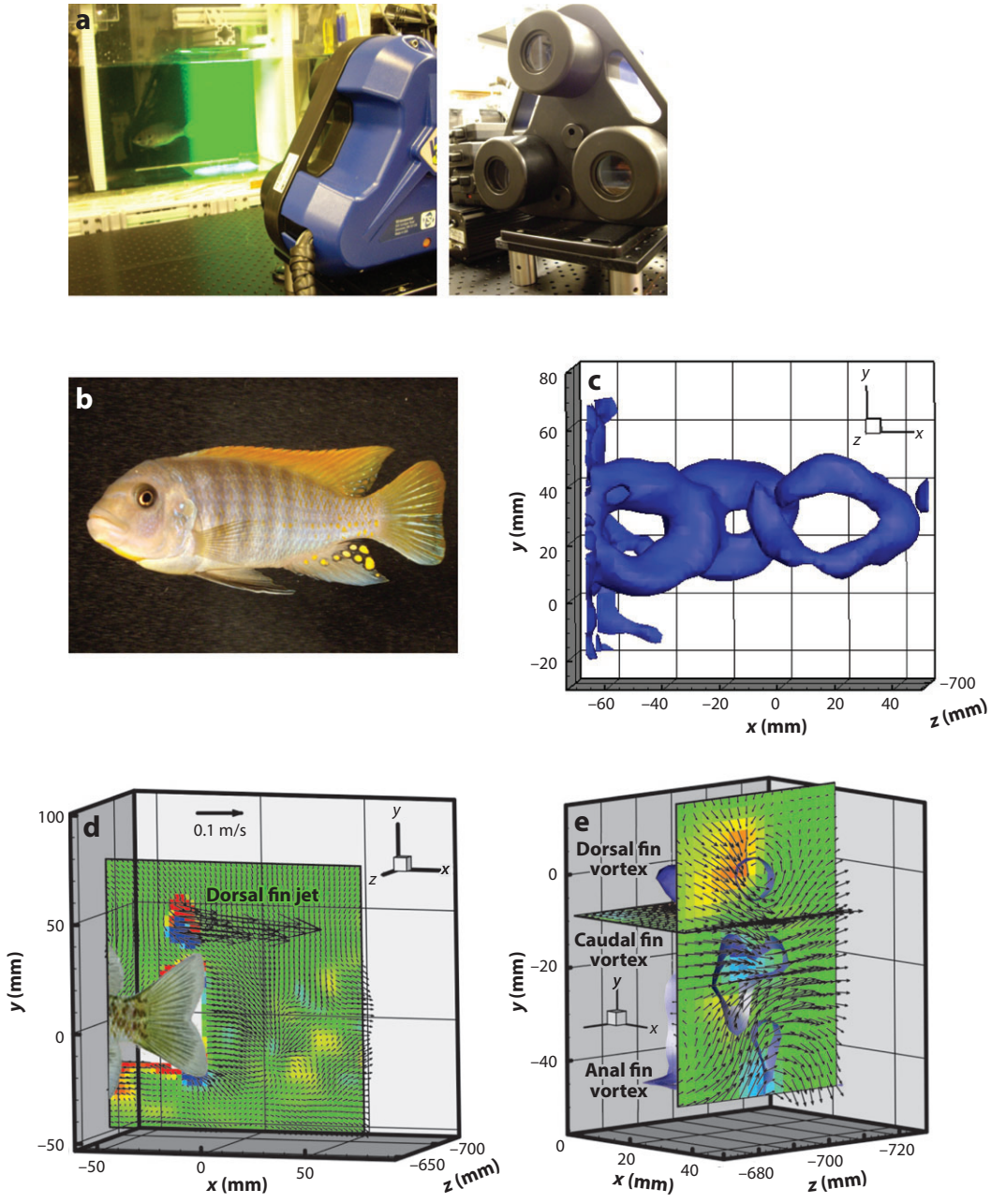

Figure 6

Patterns of water flow generated by the tail and the dorsal and anal fins of swimming teleost fish with homocercal (symmetrical) tails, as demonstrated using volumetric particle image velocimetry. (*a*) The three cameras used to reconstruct the three-dimensional flow patterns generated by the fins and body. (*b*) A cichlid fish (*Pseudotropheus greshakei*) swimming just upstream of the laser volume. (*c*) The linked-chain vortex wake produced by the cichlid's tail. (*d*) A vertical slice through the wake, illustrating the increased velocity generated by the tail and dorsal fin, contoured by *z* vorticity. (*e*) Sections through the vortex wake, showing the dorsal, caudal, and anal fin vortices in the *yz* plane and the resulting side jet (directed to the right in this figure). Figure adapted from Flammang et al. (2011a).

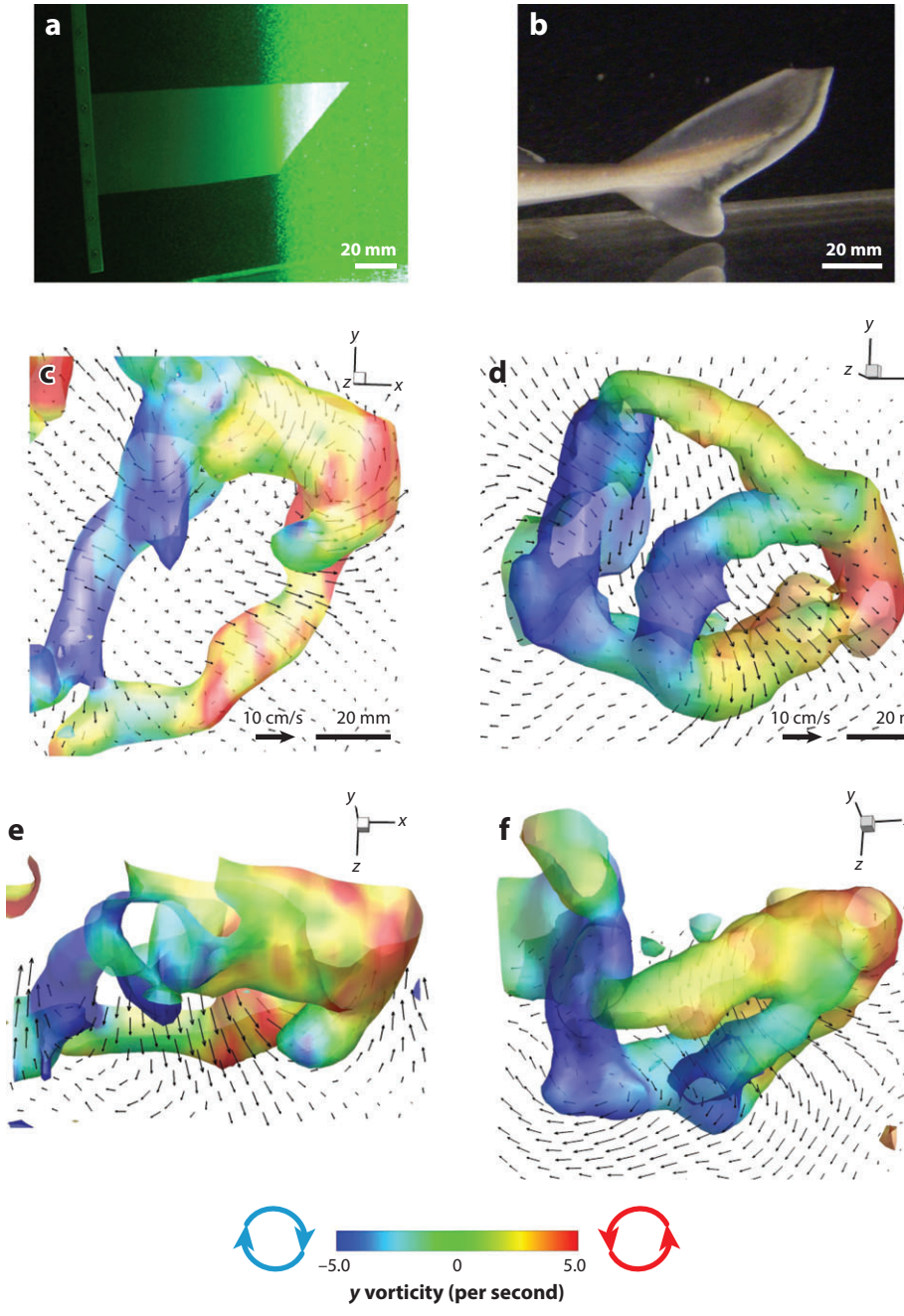

Figure 7

(*a*,*b*) Three-dimensional wakes from a simple plastic foil model of a heterocercal (asymmetrical) tail (panel *a*) and from the tail of a spiny dogfish shark (*Squalus acanthias*) (panel *b*). (*c*–*f*) Lateral or side (panels *c* and *d*, for the model and shark tails, respectively) and dorsal or overhead (panels *e* and *f*, for the model and shark tails, respectively) views of the wake structure isosurfaced by absolute vorticity and then color-coded by *y* vorticity. The lateral views include a vertical slice (*xy* plane) with velocity vectors; the dorsal views include a horizontal slice (*xz* plane) with velocity vectors. Every third velocity vector is shown for clarity. Figure adapted from Flammang et al. (2011b).

The manufacture of artificial shark skin begins with a 3D denticle model that captures the surface ridge shape and overhanging crown. The denticle model is then laid out into a 2D array, and finally the array is printed using a multimaterial 3D printer so that the denticles are manufactured of a hard material that is embedded into a flexible membrane substrate (**Figure 8*h*,*i***). Although engineers studying flow over rigid patterned surfaces have demonstrated much about the

hydrodynamic characteristics of surface structures, an essential characteristic of fish skin is that it moves as fish undulate their bodies during locomotion. If analysis of fish skin hydrodynamics is to replicate swimming conditions and flow patterns and to be biologically relevant, then analysis of fish skin function must be done under dynamic (swimming) circumstances. Static testing alone is unlikely to reveal how fish skin functions during locomotion, when complex water flows impact the skin surface and scales change their orientation and spacing as the skin bends with the flexing body.

To address this issue, we have developed a mechanical test system that generates controlled programmed movement patterns and allows the dynamic testing of biological structures under swimming conditions (Lauder et al. 2007, 2012; Quinn et al. 2014b; Wen & Lauder 2013). To study the function of shark skin denticles, we first used pieces of shark skin to construct a membrane made of this skin and attached it to a shaft that was subjected to controlled heave (side-to-side) and pitch (rotational) movements (**Figure 9**). Comparison of the swimming speed of intact shark skin membranes to membranes from which we had removed the denticles revealed an average speed increase of 12.3% (Oeffner & Lauder 2012), indicating that skin denticles improve swimming performance. Flow visualization showed that shark skin denticles alter the pattern of water flow over the skin surface compared with shark skin with the denticles removed, and suggested that, by doing so, denticles not only can reduce drag forces but also may be capable of enhancing thrust.

Testing of artificial shark skin using similar procedures and comparing smooth-surfaced membranes to biomimetic shark skin membranes with denticles (Wen et al. 2014) showed that swimming speed increases when the skin membranes are moved with moderate angular rotation (**Figure 9*b*,*c***). In addition, the presence of denticles reduced the cost of transport (energy required to travel a given distance, in joules per meter) by 5%.

These experiments illustrate the value in developing manufactured 3D models of fish skin structures that can be tested dynamically. Future progress will come in part from the ability to manipulate both the morphology of fish skin structures and the arrangement of these structures on the skin and in part from dynamic testing under conditions similar to those experienced by fish skin under natural locomotor conditions.

Energetics

In recent years, studies of the energetics of fish locomotion have provided some remarkable insights into many features of fish swimming performance. But linking the cost of locomotion to metrics of fish performance such as maneuvering ability, swimming speed, and body shape remains a challenging proposition. There is great opportunity for future work in this area, because locomotor cost is a more direct estimate of fitness than kinematic or hydrodynamic parameters, and quantifying the cost of transport provides a parameter that can be compared directly with that of robotic models.

One noteworthy area in fish swimming energetics is the analysis of eel migration and the energy stores used by eels during their 5,000–6,000-km migratory excursions (van Ginneken & van den Thillart 2000, van Ginneken et al. 2005). Van Ginneken et al. (2005) placed eels in a recirculating flow tank and allowed them to swim at speeds and for durations that approximated their months-long migration from coastal areas of North America and Europe to their breeding grounds in the Sargasso Sea. They calculated a cost of transport of approximately 0.5 kJ/kg/km, which is both a remarkably low value and substantially less than the value of 2.7 kJ/kg/km obtained from trout swimming under similar conditions. This low cost of transport for swimming eels indicates that they have more than adequate energy stores to accomplish their long migrations. Other recent fish energetics studies of note have examined fish swimming under turbulent conditions (Roche et al. 2014, Taguchi & Liao 2011), the energetics of gait transitions (Cannas

et al. 2006, Kendall et al. 2007, Korsmeyer et al. 2002), and tuna compared with non-thunniform fishes (Sepulveda & Dickson 2000, Sepulveda et al. 2003).

FISH ROBOTICS

In our effort to understand basic principles of aquatic propulsion, studying live animals is not enough. We need to be able to manipulate parameters, alter features such as stiffness, and program

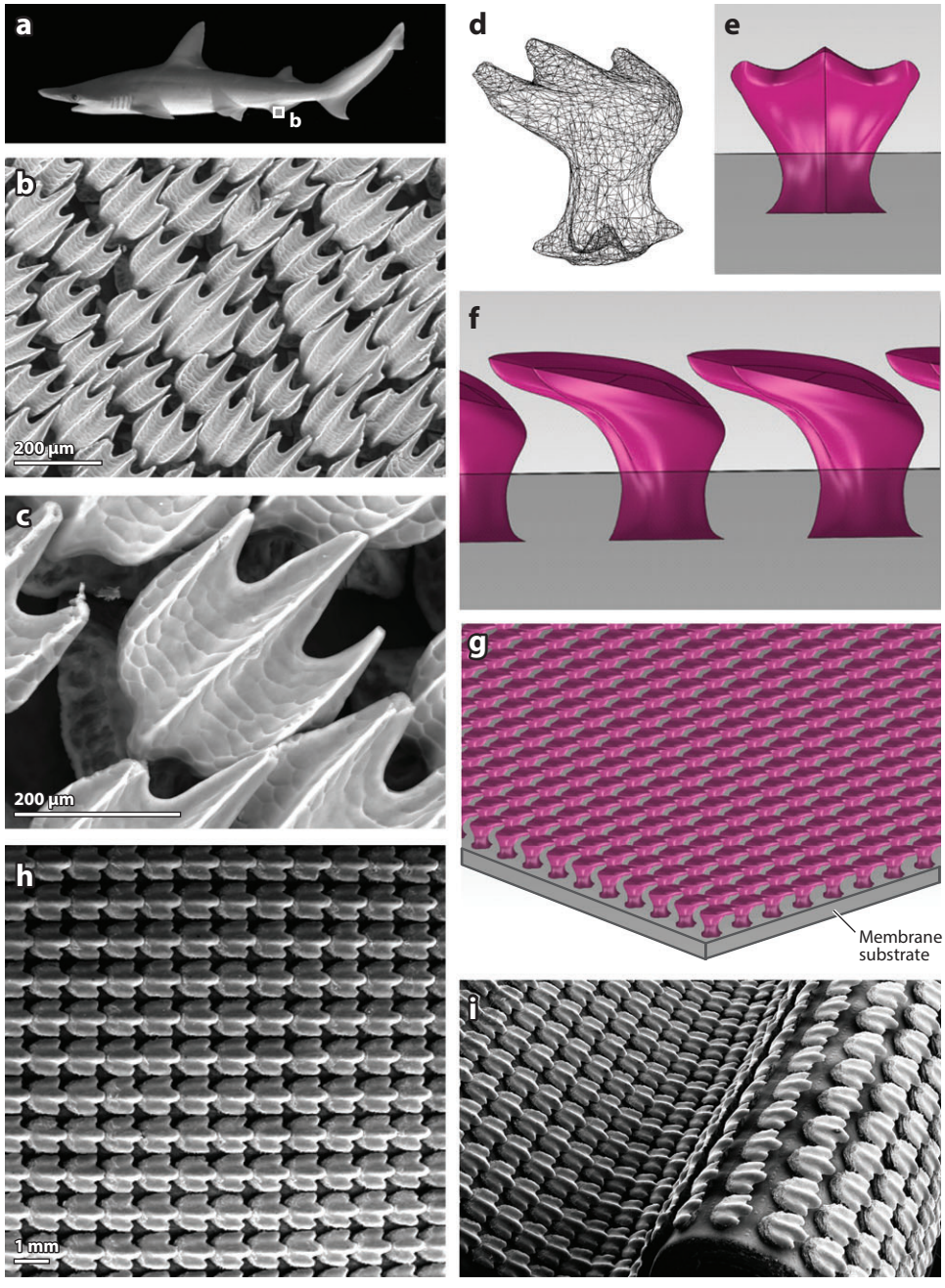

motions that are nonbiological to determine whether the fish are at a performance maximum. Robotic or mechanical devices are extremely useful in this regard and allow considerable experimental control that is not possible using only natural biological diversity.

Robotic models of fish may be complex (**Figure 10**) and provide at least a somewhat realistic imitation of biological reality. Such robotic devices can be quite challenging to build, control, and test, but they are less subject to the criticisms aimed at simpler robotic devices that could be viewed as being too far removed from "real" fish structure and function to be informative. The complexity of such mechanical devices does limit our ability to iterate design changes and conduct replicate tests with varying structures.

Robotic or mechanical models may also consist of test platforms or considerably simplified representations of fish reality (**Figure 11**). Such mechanical platforms can represent fin-like structures that model whole fish fins (Esposito et al. 2012, Tangorra et al. 2011b) or can represent simple flexible propulsive surfaces that vary in stiffness or the shape of the model tail's trailing edge. Although obviously not as representational of fish biology, simple robotic systems have the advantage of being easy to reconfigure in order to alter properties such as stiffness and shape, and they facilitate comprehensive testing that can include force and torque measurement, flow visualization, and the calculation of key locomotor metrics such as the cost of transport and the power requirements of swimming (Alben et al. 2012; Lauder et al. 2011a, 2012; Long 2012; Wen & Lauder 2013). Surprisingly, even very simple robotic models have proven to display many of the locomotor properties of undulating live fish (Shelton et al. 2014).

Simple robotic models of aquatic propulsion have provided data that address several key biomechanical issues, and some interesting results have come from very simple experiments. For example, measurements of the swimming speeds of flexible materials that are identical except for their flexural stiffnesses have shown that there can be an optimum stiffness at which swimming speed is maximized for a given motion program, but changing the swimming motion can eliminate this optimum and produce a broad plateau over which stiffness has relatively little effect (**Figure 12*a***). Fish may take advantage of such a plateau by altering the pattern of muscular activation of body segments to minimize the performance loss that would otherwise occur. Testing of more complicated fish fin models, in which the flexural stiffness of the individual fin rays that actuate the fin surface is altered (**Figure 12*b***), has shown that fin supports can be either too flexible or too stiff to generate maximal thrust forces and that stiffness has a complex interaction with frequency: The optimal stiffness of fish fin models changes with the flapping frequency. Because fish are able to

←

Figure 8

Environmental scanning electron microscope images of the denticles (or scales) on the skin of a bonnethead shark (*Sphyrna tiburo*) and manufactured biomimetic model shark skin. (*a*) A bonnethead shark swimming in a laboratory flow tank. (*b*) A view of skin denticles near the anal fin. (*c*) A closer view of these same scales to show the three prominent ridges. (*d*) A three-dimensional model of an individual denticle, showing the ridged surface and the stalk; the base of this stalk is embedded into the skin of a shark. (*e*) A model of an individual solid denticle. (*f*) A row of denticles, showing how the top of one denticle overlaps the base of the adjacent one. (*g*) A two-dimensional denticle array in which rigid denticles are laid out on a flexible membrane substrate. (*h*,*i*) Fabricated biomimetic synthetic shark skin membranes used for hydrodynamic testing. Artificial shark skin is produced using additive manufacturing. Membranes are shown in flat (panel *h*) and curved (panel *i*) configurations to illustrate how the rigid denticles are embedded into a flexible membrane. Note the change in relative spacing among denticles in the convex and concave regions of the curved membrane (panel *i*). Panels *a–c* adapted from Oeffner & Lauder (2012); panels *d–i* adapted from Wen et al. (2014).

actively alter the stiffness of the fin rays that support the fin membrane, this capability may allow fish to achieve efficient locomotion over a range of speeds.

Simple experiments such as changing the length of a swimming object can reveal unexpected effects (Alben et al. 2012, Quinn et al. 2014b). A flexing swimming body may interact with the surrounding fluid to produce resonant modes that generate substantial fluctuations in swimming speed as the length of the foil is changed (**Figure 12*c*,*d***). Even small length changes, on the order of 10%, can change swimming speed by a factor of three to five times. Resonant phenomena such as this have yet to be exploited in the design of aquatic robots.

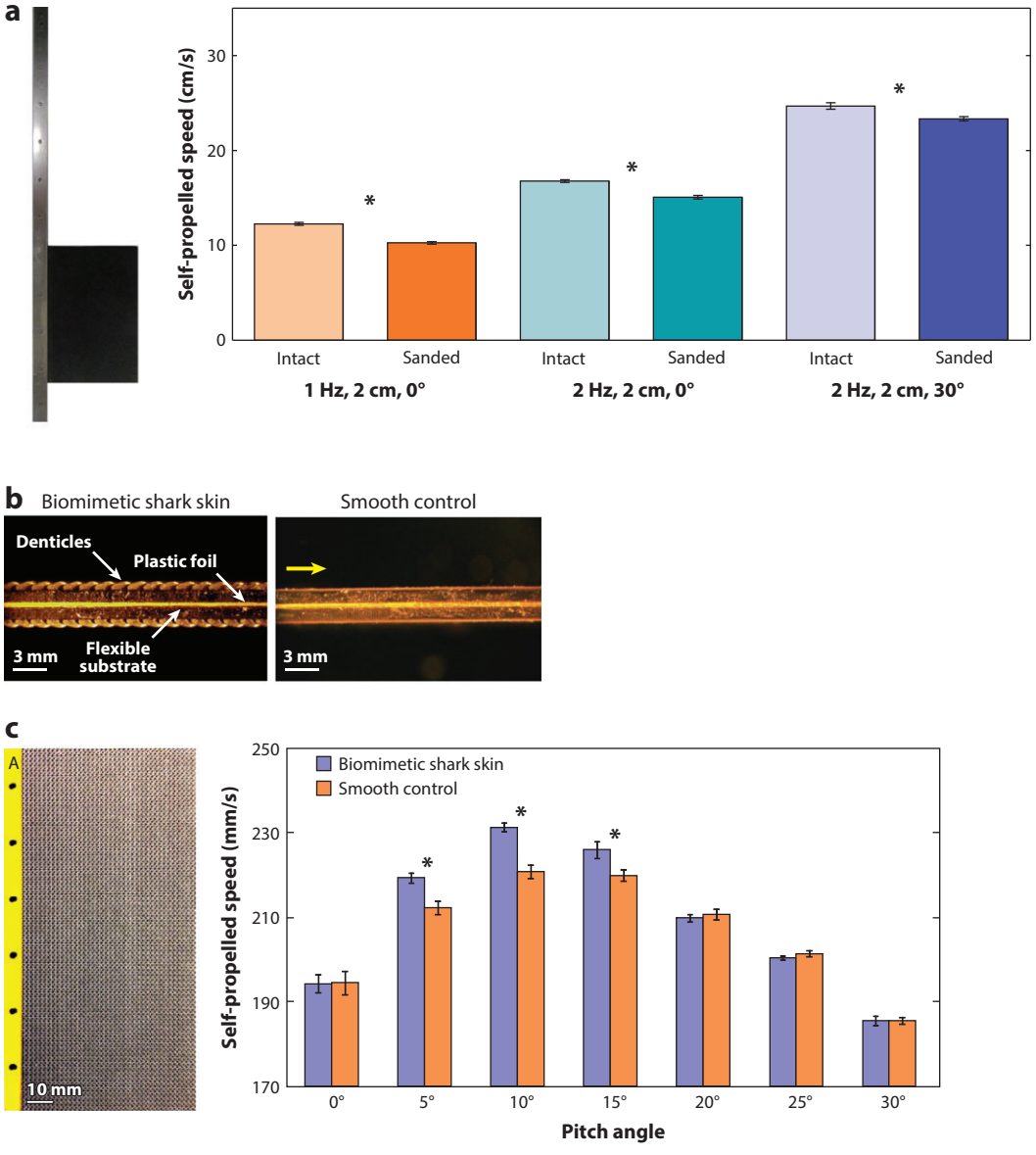

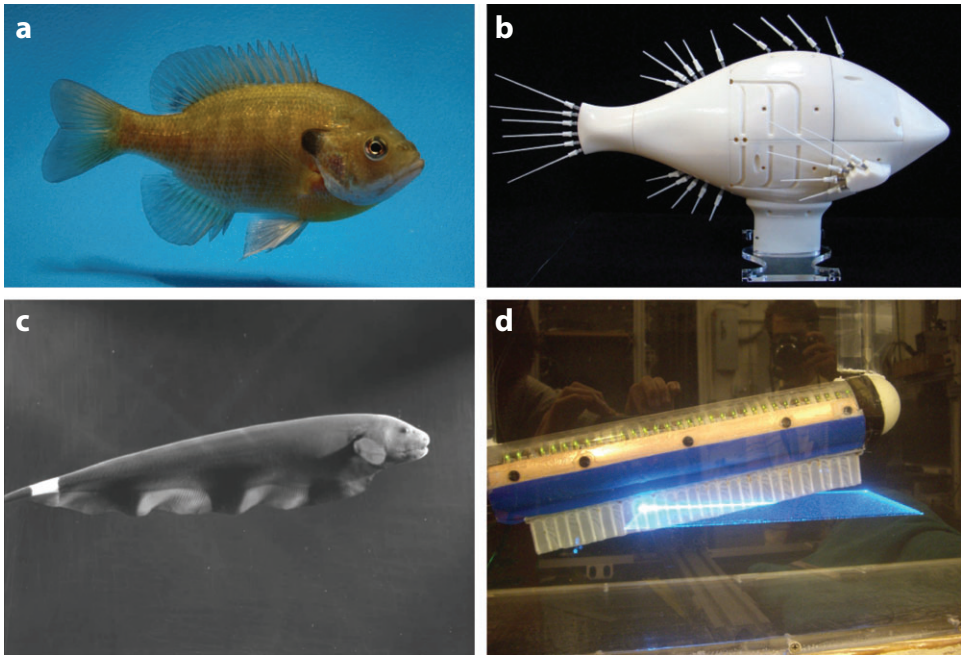

Figure 10

Complex robotic models of fish propulsion along with their biological models. (*a*) A bluegill sunfish (*Lepomis macrochirus*), a species often used for studying fin-based swimming as well as undulatory propulsion. (*b*) A robotic bluegill sunfish with actuated pectoral, caudal, dorsal, and anal fins (the fin ray skeleton is displayed for each fin; the covering material has been removed). In this robotic model, the body is stiff and houses the actuators. (*c*) A ghost knifefish (*Apteronotus albifrons*), showing the elongate anal fin, which can generate wave-like motions to power propulsion and maneuvering. (*d*) A robotic ghost knifefish model with an elongate flexible anal fin. In this image, the anal fin model is placed in a laser light sheet to image wake flow patterns. Panel *b* adapted from Tangorra et al. (2011a); panel *d* adapted from Curet et al. (2011a,b).

←

Figure 9

The hydrodynamic function of shark skin and biomimetic models. (*a*) Dynamic testing of the hydrodynamic function of shark skin denticles using pieces of shark skin that are attached to a flat support (*left*), which in turn is attached to a mechanical flapping foil device that allows controlled heave (side-to-side) and pitch (rotational) movements of the shark skin membrane. The graph (*right*) shows the self-propelled swimming speeds of the shark skin membrane with intact denticles and after the denticles have been sanded off (to produce a relatively smooth surface) under three different motion programs. Note that, in each case, the swimming speed of the shark skin was significantly greater with the denticles intact (*asterisks*) than it was after the denticles were removed by sanding. (*b*) An edge-on view of biomimetic shark skin assembled into a two-layer membrane compared with a smooth control of the same mass. A central yellow plastic element supports the two flexible membranes. (*c*) The completed assembly of the tested flexible biomimetic shark skin foil (*left*). A flat support attaches to the yellow area with holes on the left side of the foil, and this support is moved by a mechanical flapping device. The graph (*right*) shows the results from testing the self-propelled swimming speed of the biomimetic shark skin foil and the smooth control at different pitch angles. Error bars represent ± 1 standard error of the mean. At pitch angles of 5°, 10°, and 15° (*asterisks*), the swimming speeds of the biomimetic shark skin foils were significantly greater than those of the smooth controls; at the other four pitch angles, the swimming speeds were similar. Panel *a* adapted from Oeffner & Lauder (2012); panels *b* and *c* adapted from Wen et al. (2014).

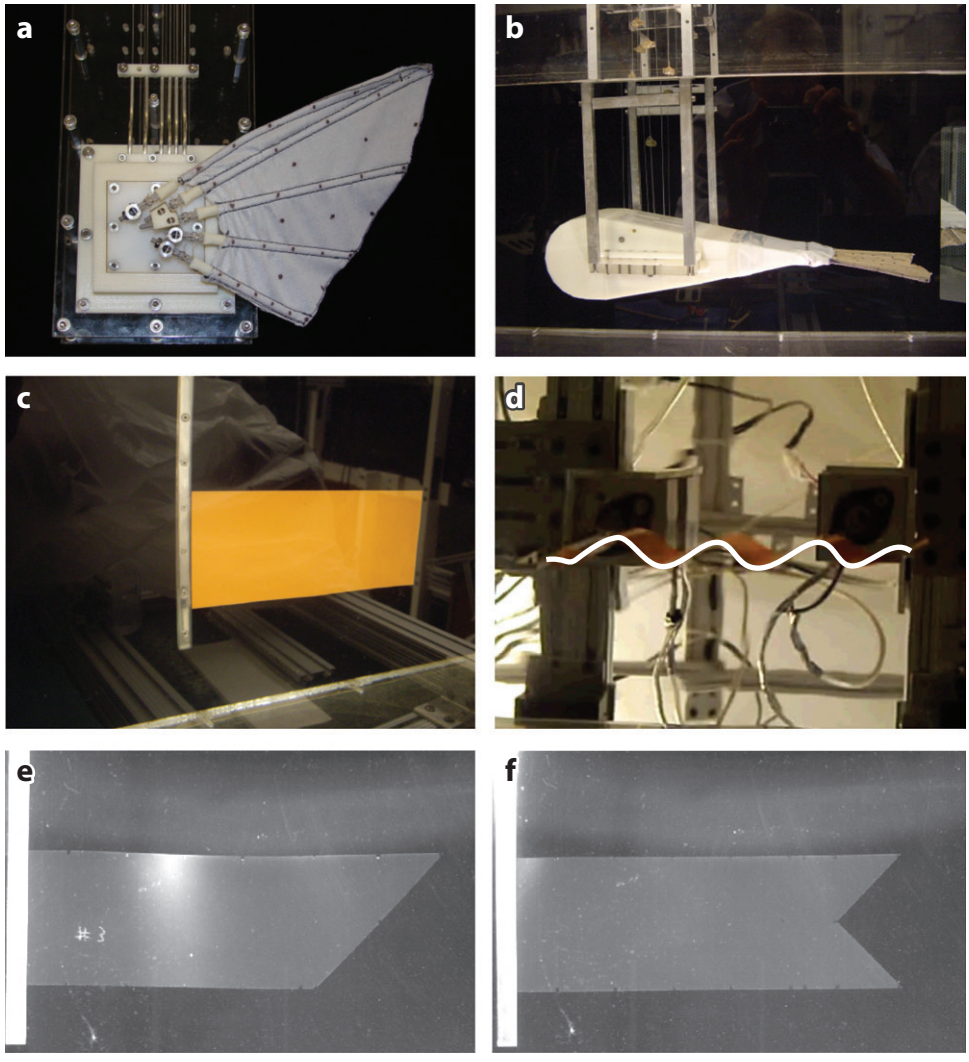

Figure 11

A selection of aquatic robotic test platforms designed to represent aspects of the functional design of swimming fish. (*a*) A robotic fish pectoral fin. (*b*) A robotic fish caudal fin with a streamlined rigid body to support the fin. (*c*) A flexible flapping foil under robotic control. The leading edge can be moved in heave (side-to-side) and pitch (rotational) motions. (*d*) A flexible foil swimming under heave actuation of the leading edge (to the left), showing the ribbon shape assumed by the foil during locomotion. A white line has been added to enhance the visibility of the foil shape. (*e*,*f*) Flexible swimming foils with two trailing edge configurations (with the same surface area) to mimic different fish tail shapes. These foils swim at different speeds. Panel *a* adapted from Tangorra et al. (2010); panel *b* adapted from Esposito et al. (2012); panels *c* and *d* adapted from Lauder et al. (2011b); panels *e* and *f* adapted from Lauder et al. (2012).

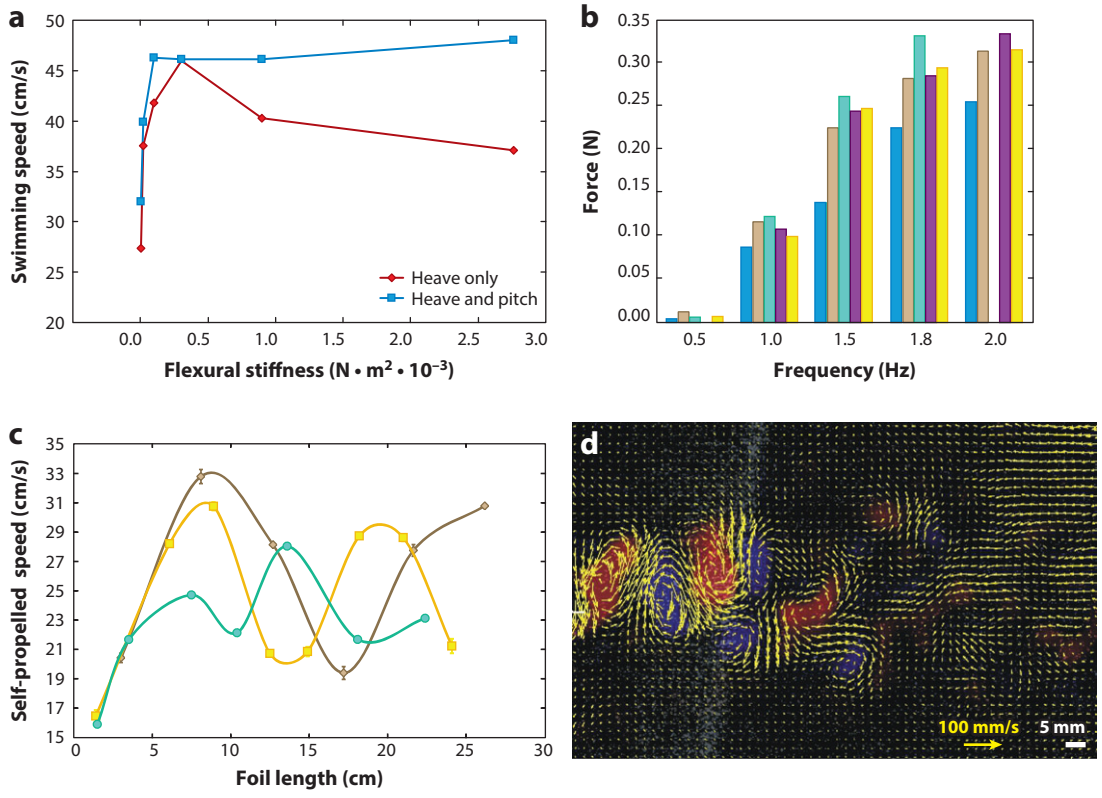

Figure 12

Data from robotic test platforms illustrating several key features of aquatic propulsive systems. (*a*) The effects of the flexural stiffness of a bending body on swimming speed. If the leading edge is actuated in heave (side-to-side) motion only, there is a distinct performance peak. If pitch (rotational) motion is added, that peak is replaced by a broad plateau. (*b*) Mean thrust forces produced by robotic fish tails with different stiffnesses. From left to right at each frequency, the bars represent tails of increasing stiffness. (*c*) The effects of changing the length of a swimming foil on swimming speed. The three curves represent foils of different stiffnesses; the foils were actuated in heave at the leading edge only. (*d*) Wake flow pattern measured behind a swimming foil similar to that shown in **Figure 11*c***. This flow pattern closely mimics that of a freely swimming fish. The yellow arrows indicate water velocity, and the red and blue colors represent opposite-sign vorticity. Panel *a* adapted from Lauder et al. (2011b); panel *b* adapted from Esposito et al. (2012); panel *c* adapted from Lauder et al. (2012); panel *d* adapted from Lauder et al. (2011a).

Finally, simple robotic models of fish swimming near substrates have proven useful in understanding the physics of the interactions between a flexible swimming object and a nearby solid surface (Blevins & Lauder 2013, Quinn et al. 2014a,c).

FISH LOCOMOTION AND OCEAN MIXING

Vorticity in the wake of biological swimmers is of interest beyond fluid dynamicists and biomechanists seeking to understand the physics of aquatic propulsion. The propulsion of fish and other organisms in the ocean has been implicated as a significant factor in ocean mixing, a key process underlying ocean dynamics (Dewar et al. 2006, Katija 2012, Katija & Dabiri 2009). Individual fish shed a distinct vortex wake, and fishes, whether in a school or not, introduce substantial circulation into ocean waters owing to their enormous biomass and migratory patterns. Although the focus

of most research has been on plankton and jellyfish locomotor effects on ocean mixing, there is no doubt that fish swimming in schools and the large biomass associated with the diel migration of fishes such as lantern fish have considerable effects on fluid layers in the ocean and introduce considerable energy that contributes to the mixing of nutrients and temperature. The extent to which overfishing and the substantial depletion of fish biomass have altered ocean dynamics by removing a key mixing factor has yet to be determined, but the effect may be substantial.

DISCLOSURE STATEMENT

The author is not aware of any affiliations, memberships, funding, or financial holdings that might be perceived as affecting the objectivity of this review.

ACKNOWLEDGMENTS

The research reported here was supported by Office of Naval Research grant N00014-09-1-0352, monitored by Dr. Thomas McKenna, and by National Science Foundation grants IBN0316675 and EFRI-0938043. Additional support was provided by ONR MURI award N000141410533, monitored by Dr. Bob Brizzolara. Many thanks to Nicole Danos, Brooke Flammang, James Tangorra, Erik Anderson, Erin Blevins, Jeanette Lim, Oscar Curet, Malcolm MacIver, Dan Quinn, Patrick Thornycroft, Grace Xiong, Ryan Shelton, and Klea Kalionzes for collaboration on experiments and for numerous helpful discussions on bio-inspired propulsion.

LITERATURE CITED

Alben S, Madden PG, Lauder GV. 2007. The mechanics of active fin-shape control in ray-finned fishes. *J. R. Soc. Interface* 4:243–56

Alben S, Witt C, Baker TV, Anderson EJ, Lauder GV. 2012. Dynamics of freely swimming flexible foils. *Phys. Fluids* 24:051901

Alexander RM. 1967. *Functional Design in Fishes*. London: Hutchinson

Alexander RM. 1983. The history of fish mechanics. See Webb & Weihs 1983, pp. 1–35

Anderson EJ, McGillis W, Grosenbaugh MA. 2001. The boundary layer of swimming fish. *J. Exp. Biol.* 204:81–102

Blake RW. 1983. *Fish Locomotion*. Cambridge, UK: Cambridge Univ. Press

Blevins EL, Lauder GV. 2012. Rajiform locomotion: three-dimensional kinematics of the pectoral fin surface during swimming by the freshwater stingray *Potamotrygon orbignyi*. *J. Exp. Biol.* 215:3231–41

Blevins EL, Lauder GV. 2013. Swimming near the substrate: a simple robotic model of stingray locomotion. *Bioinspir. Biomim.* 8:016005

Borazjani I, Sotiropoulos F. 2009. Numerical investigation of the hydrodynamics of anguilliform swimming in the transitional and inertial flow regimes. *J. Exp. Biol.* 212:576–92

Borazjani I, Sotiropoulos F, Tytell ED, Lauder GV. 2012. On the hydrodynamics of the bluegill sunfish C-start escape response: three-dimensional simulations and comparison with experimental data. *J. Exp. Biol.* 215:671–84

Borelli GA. 1680. *On the Movement of Animals*. Transl. 1989 by P Maquet. Berlin: Springer-Verlag

Bozkurttas M, Mittal R, Dong H, Lauder GV, Madden PGA. 2009. Low-dimensional models and performance scaling of a highly deformable fish pectoral fin. *J. Fluid Mech.* 631:311–42

Brainerd E, Page B, Fish F. 1997. Opercular jetting during fast-starts by flatfishes. *J. Exp. Biol.* 200:1179–88

Bruet BJF, Song J, Boyce MC, Ortiz C. 2008. Materials design principles of ancient fish armour. *Nat. Mater.* 7:748–56

Cannas M, Schaefer J, Domenici P, Steffensen JF. 2006. Gait transition and oxygen consumption in swimming striped surfperch *Embiotoca lateralis* Agassiz. *J. Fish Biol.* 69:1612–25

Carlson RL, Lauder GV. 2010. Living on the bottom: kinematics of benthic station-holding in darter fishes (Percidae: Etheostomatinae). *J. Morphol.* 271:25–35
Carlson RL, Lauder GV. 2011. Escaping the flow: boundary layer use by the darter *Etheostoma tetrazonum* (Percidae) during benthic station holding. *J. Exp. Biol.* 214:1181–93
Castro JI. 2011. *The Sharks of North America*. Oxford, UK: Oxford Univ. Press
Curet OM, Patankar NA, Lauder GV, MacIver MA. 2011a. Aquatic manoeuvering with counter-propagating waves: a novel locomotive strategy. *J. R. Soc. Interface* 8:1041–50
Curet OM, Patankar NA, Lauder GV, MacIver MA. 2011b. Mechanical properties of a bio-inspired robotic knifefish with an undulatory propulsor. *Bioinspir. Biomim.* 6:026004
Dewar WK, Bingham R, Iverson R, Nowacek DP, St Laurent LC, Wiebe PH. 2006. Does the marine biosphere mix the ocean? *J. Mar. Res.* 64:541–61
Domenici P, Blake RW. 1997. The kinematics and performance of fish fast-start swimming. *J. Exp. Biol.* 200:1165–78
Domenici P, Kapoor BG, eds. 2010. *Fish Locomotion: An Eco-Ethological Perspective*. Enfield, NH: Science
Dong H, Bozkurttas M, Mittal R, Madden P, Lauder GV. 2010. Computational modeling and analysis of the hydrodynamics of a highly deformable fish pectoral fin. *J. Fluid Mech.* 645:345–73
Donley J, Dickson KA. 2000. Swimming kinematics of juvenile Kawakawa tuna (*Euthynnus affinis*) and chub mackerel (*Scomber japonicus*). *J. Exp. Biol.* 203:3103–16
Donley J, Shadwick R. 2003. Steady swimming muscle dynamics in the leopard shark *Triakis semifasciata*. *J. Exp. Biol.* 206:1117–26
Drucker EG. 1996. The use of gait transition speed in comparative studies of fish locomotion. *Am. Zool.* 36:555–66
Drucker EG, Jensen J. 1996. Pectoral fin locomotion in the striped surfperch. I. Kinematic effects of swimming speed and body size. *J. Exp. Biol.* 199:2235–42
Drucker EG, Lauder GV. 1999. Locomotor forces on a swimming fish: three-dimensional vortex wake dynamics quantified using digital particle image velocimetry. *J. Exp. Biol.* 202:2393–412
Drucker EG, Lauder GV. 2000. A hydrodynamic analysis of fish swimming speed: wake structure and locomotor force in slow and fast labriform swimmers. *J. Exp. Biol.* 203:2379–93
Drucker EG, Lauder GV. 2002. Experimental hydrodynamics of fish locomotion: functional insights from wake visualization. *Integr. Comp. Biol.* 42:243–57
Drucker EG, Lauder GV. 2005. Locomotor function of the dorsal fin in rainbow trout: kinematic patterns and hydrodynamic forces. *J. Exp. Biol.* 208:4479–94
Drucker EG, Walker JA, Westneat MW. 2006. Mechanics of pectoral fin swimming in fishes. See Shadwick & Lauder 2006, pp. 369–423
Eaton RC, Bombardieri RA, Meyer D. 1977. The Mauthner initiated startle response in teleost fish. *J. Exp. Biol.* 66:65–81
Eaton RC, DiDomenico R. 1986. Role of the teleost escape response during development. *Trans. Am. Fish. Soc.* 115:128–42
Ellerby DJ, Gerry SP. 2011. Sympatric divergence and performance trade-offs of bluegill ecomorphs. *Evol. Biol.* 38:422–33
Esposito C, Tangorra JL, Flammang BE, Lauder GV. 2012. A robotic fish caudal fin: effects of stiffness and motor program on locomotor performance. *J. Exp. Biol.* 215:56–67
Ferry LA, Lauder GV. 1996. Heterocercal tail function in leopard sharks: a three-dimensional kinematic analysis of two models. *J. Exp. Biol.* 199:2253–68
Fish F, Lauder GV. 2006. Passive and active flow control by swimming fishes and mammals. *Annu. Rev. Fluid Mech.* 38:193–224
Fish F, Lauder GV. 2013. Not just going with the flow. *Am. Sci.* 101:114–23
Flammang BE, Alben S, Madden PGA, Lauder GV. 2013. Functional morphology of the fin rays of teleost fishes. *J. Morphol.* 274:1044–59
Flammang BE, Lauder GV. 2013. Pectoral fins aid in navigation of a complex environment by bluegill sunfish under sensory deprivation conditions. *J. Exp. Biol.* 216:3084–89
Flammang BE, Lauder GV, Troolin DR, Strand T. 2011a. Volumetric imaging of fish locomotion. *Biol. Lett.* 7:695–98

Flammang BE, Lauder GV, Troolin DR, Strand T. 2011b. Volumetric imaging of shark tail hydrodynamics reveals a three-dimensional dual-ring vortex wake structure. *Proc. R. Soc. B* 278:3670–78
Gerstner CL. 1998. Use of substratum ripples for flow refuging by Atlantic cod, *Gadus morhua*. *Environ. Biol. Fishes* 51:455–60
Gerstner CL, Webb PW. 1998. The station-holding performance of the plaice *Pleuronectes platessa* on artificial substratum ripples. *Can. J. Zool.* 76:260–68
Gibb A, Jayne BC, Lauder GV. 1994. Kinematics of pectoral fin locomotion in the bluegill sunfish *Lepomis macrochirus*. *J. Exp. Biol.* 189:133–61
Gillis GB. 1996. Undulatory locomotion in elongate aquatic vertebrates: anguilliform swimming since Sir James Gray. *Am. Zool.* 36:656–65
Gillis GB. 1997. Anguilliform locomotion in an elongate salamander (*Siren intermedia*): effects of speed on axial undulatory movements. *J. Exp. Biol.* 200:767–84
Goodrich ES. 1930. *Studies on the Structure and Development of Vertebrates*. London: Macmillan
Gray J. 1933a. Studies in animal locomotion. I. The movement of fish with special reference to the eel. *J. Exp. Biol.* 10:88–104
Gray J. 1933b. Studies in animal locomotion. II. The relationship between waves of muscular contraction and the propulsive mechanism of the eel. *J. Exp. Biol.* 10:386–90
Gray J. 1933c. Studies in animal locomotion. III. The propulsive mechanism of the whiting (*Gadus merlangus*). *J. Exp. Biol.* 10:391–400
Gray J. 1953. The locomotion of fishes. In *Essays in Marine Biology*, ed. SM Marshall, AP Orr, pp. 1–16. Edinburgh, Scotl.: Oliver & Boyd
Gray J. 1968. *Animal Locomotion*. London: Weidenfeld & Nicolson
Hale ME, Day RD, Thorsen DH, Westneat MW. 2006. Pectoral fin coordination and gait transitions in steadily swimming juvenile reef fishes. *J. Exp. Biol.* 209:3708–18
Hale ME, Long JH Jr, McHenry MJ, Westneat MW. 2002. Evolution of behavior and neural control of the fast-start escape response. *Evolution* 56:993–1007
Hess F, Videler JJ. 1984. Fast continuous swimming of saithe (*Pollachius virens*): a dynamic analysis of bending moments and muscle power. *J. Exp. Biol.* 109:229–51
Jagnandan K, Sanford CP. 2013. Kinematics of ribbon-fin locomotion in the bowfin, *Amia calva*. *J. Exp. Zool. A* 319:569–83
Katija K. 2012. Biogenic inputs to ocean mixing. *J. Exp. Biol.* 215:1040–49
Katija K, Dabiri JO. 2009. A viscosity-enhanced mechanism for biogenic ocean mixing. *Nature* 460:624–26
Kendall JL, Lucey KS, Jones EA, Wang J, Ellerby DJ. 2007. Mechanical and energetic factors underlying gait transitions in bluegill sunfish (*Lepomis macrochirus*). *J. Exp. Biol.* 210:4265–71
Kern S, Koumoutsakos P. 2006. Simulations of optimized anguilliform swimming. *J. Exp. Biol.* 209:4841–57
Korsmeyer K, Steffensen J, Herskin J. 2002. Energetics of median and paired fin swimming, body and caudal fin swimming, and gait transition in parrotfish (*Scarus schlegeli*) and triggerfish (*Rhinecanthus aculeatus*). *J. Exp. Biol.* 205:1253–63
Lauder GV. 2006. Locomotion. In *The Physiology of Fishes*, ed. DH Evans, JB Claiborne, pp. 3–46. Boca Raton, FL: CRC. 3rd ed.
Lauder GV, Anderson EJ, Tangorra JL, Madden PGA. 2007. Fish biorobotics: kinematics and hydrodynamics of self-propulsion. *J. Exp. Biol.* 210:2767–80
Lauder GV, Drucker EG. 2002. Forces, fishes, and fluids: hydrodynamic mechanisms of aquatic locomotion. *News Physiol. Sci.* 17:235–40
Lauder GV, Flammang BE, Alben S. 2012. Passive robotic models of propulsion by the bodies and caudal fins of fish. *Integr. Comp. Biol.* 52:576–87
Lauder GV, Lim J, Shelton R, Witt C, Anderson EJ, Tangorra JL. 2011a. Robotic models for studying undulatory locomotion in fishes. *Mar. Technol. Soc. J.* 45:41–55
Lauder GV, Madden PGA. 2006. Learning from fish: kinematics and experimental hydrodynamics for roboticists. *Int. J. Autom. Comput.* 4:325–35
Lauder GV, Madden PGA. 2008. Advances in comparative physiology from high-speed imaging of animal and fluid motion. *Annu. Rev. Physiol.* 70:143–63

Lauder GV, Madden PGA, Mittal R, Dong H, Bozkurttas M. 2006. Locomotion with flexible propulsors I: experimental analysis of pectoral fin swimming in sunfish. *Bioinspir. Biomim.* 1:S25–34
Lauder GV, Madden PGA, Tangorra JL, Anderson E, Baker TV. 2011b. Bioinspiration from fish for smart material design and function. *Smart Mater. Struct.* 20:094014
Lauder GV, Tytell ED. 2006. Hydrodynamics of undulatory propulsion. See Shadwick & Lauder 2006, pp. 425–68
Liao JC. 2007. A review of fish swimming mechanics and behaviour in altered flows. *Philos. Trans. R. Soc. Lond. B* 362:1973–93
Liao JC, Beal DN, Lauder GV, Triantafyllou MS. 2003a. Fish exploiting vortices decrease muscle activity. *Science* 302:1566–69
Liao JC, Beal DN, Lauder GV, Triantafyllou MS. 2003b. The Kármán gait: novel body kinematics of rainbow trout swimming in a vortex street. *J. Exp. Biol.* 206:1059–73
Lighthill J. 1975. *Mathematical Biofluiddynamics*. Philadelphia: Soc. Ind. Appl. Math.
Long J. 2012. *Darwin's Devices: What Evolving Robots Can Teach Us About the History of Life and the Future of Technology*. New York: Basic
Macesic LJ, Mulvaney D, Blevins EL. 2013. Synchronized swimming: coordination of pelvic and pectoral fins during augmented punting by the freshwater stingray *Potamotrygon orbignyi*. *Zoology* 116:144–50
Maddock L, Bone Q, Rayner JMV, eds. 1994. *Mechanics and Physiology of Animal Swimming*. Cambridge, UK: Cambridge Univ. Press
Maia A, Wilga C. 2013a. Anatomy and muscle activity of the dorsal fins in bamboo sharks and spiny dogfish during turning maneuvers. *J. Morphol.* 274:1288–98
Maia A, Wilga C. 2013b. Function of dorsal fins in bamboo shark during steady swimming. *Zoology* 116:224–31
Maia A, Wilga C, Lauder GV. 2012. Biomechanics of locomotion in sharks, rays and chimeras. In *Biology of Sharks and Their Relatives*, ed. JC Carrier, JA Musick, MR Heithaus, pp. 125–51. Boca Raton, FL: CRC. 2nd ed.
Motta P, Habegger ML, Lang A, Hueter R, Davis J. 2012. Scale morphology and flexibility in the shortfin mako *Isurus oxyrinchus* and the blacktip shark *Carcharhinus limbatus*. *J. Morphol.* 273:1096–110
Müller UK, Stamhuis E, Videler J. 2002. Riding the waves: the role of the body wave in undulatory fish swimming. *Integr. Comp. Biol.* 42:981–87
Müller UK, van den Boogaart JGM, van Leeuwen JL. 2008. Flow patterns of larval fish: undulatory swimming in the intermediate flow regime. *J. Exp. Biol.* 211:196–205
Nauen JC, Lauder GV. 2002. Hydrodynamics of caudal fin locomotion by chub mackerel, *Scomber japonicus* (Scombridae). *J. Exp. Biol.* 205:1709–24
Oeffner J, Lauder GV. 2012. The hydrodynamic function of shark skin and two biomimetic applications. *J. Exp. Biol.* 215:785–95
Peng J, Dabiri JO, Madden PG, Lauder GV. 2007. Non-invasive measurement of instantaneous forces during aquatic locomotion: a case study of the bluegill sunfish pectoral fin. *J. Exp. Biol.* 210:685–98
Phelan C, Tangorra JL, Lauder GV, Hale ME. 2010. A biorobotic model of the sunfish pectoral fin for investigations of fin sensorimotor control. *Bioinspir. Biomim.* 5:035003
Quinn DB, Lauder GV, Smits AJ. 2014a. Flexible propulsors in ground effect. *Bioinspir. Biomim.* 9:036008
Quinn DB, Lauder GV, Smits AJ. 2014b. Scaling the propulsive performance of heaving flexible panels. *J. Fluid Mech.* 738:250–67
Quinn DB, Moored KW, Dewey PA, Smits AJ. 2014c. Unsteady propulsion near a solid boundary. *J. Fluid Mech.* 742:152–70
Roche DG, Taylor MK, Binning SA, Johansen JL, Domenici P, Steffensen JF. 2014. Unsteady flow affects swimming energetics in a labriform fish (*Cymatogaster aggregata*). *J. Exp. Biol.* 217:414–22
Rosenberger L. 2001. Pectoral fin locomotion in batoid fishes: undulation *versus* oscillation. *J. Exp. Biol.* 204:379–94
Rosenberger L, Westneat MW. 1999. Functional morphology of undulatory pectoral fin locomotion in the stingray *Taeniura lymma* (Chondrichthyes: Dasyatidae). *J. Exp. Biol.* 202:3523–39
Ruiz-Torres R, Curet OM, Lauder GV, MacIver MA. 2013. Kinematics of the ribbon fin in hovering and swimming of the electric ghost knifefish. *J. Exp. Biol.* 216:823–34

Sepulveda C, Dickson KA. 2000. Maximum sustainable speeds and cost of swimming in juvenile Kawakawa tuna (*Euthynnus affinis*) and chub mackerel (*Scomber japonicus*). *J. Exp. Biol.* 203:3089–101
Sepulveda C, Dickson KA, Graham JB. 2003. Swimming performance studies on the eastern Pacific bonito *Sarda chiliensis*, a close relative of the tunas (family Scombridae) II. Energetics. *J. Exp. Biol.* 206:2739–48
Sfakiotakis M, Lane D, Davies JB. 1999. Review of fish swimming modes for aquatic locomotion. *IEEE J. Ocean. Eng.* 24:237–52
Shadwick RE, Gemballa S. 2006. Structure, kinematics, and muscle dynamics in undulatory swimming. See Shadwick & Lauder 2006, pp. 241–80
Shadwick RE, Goldbogen JA. 2012. Muscle function and swimming in sharks. *J. Fish Biol.* 80:1904–39
Shadwick RE, Lauder GV, eds. 2006. *Fish Biomechanics*. Fish Physiol. Vol. 23. San Diego, CA: Academic
Shelton RM, Thornycroft P, Lauder GV. 2014. Undulatory locomotion by flexible foils as biomimetic models for understanding fish propulsion. *J. Exp. Biol.* 217:2110–20
Standen EM. 2008. Pelvic fin locomotor function in fishes: three-dimensional kinematics in rainbow trout (*Oncorhynchus mykiss*). *J. Exp. Biol.* 211:2931–42
Standen EM. 2010. Muscle activity and hydrodynamic function of pelvic fins in trout (*Oncorhynchus mykiss*). *J. Exp. Biol.* 213:831–41
Standen EM, Lauder GV. 2005. Dorsal and anal fin function in bluegill sunfish *Lepomis macrochirus*: three-dimensional kinematics during propulsion and maneuvering. *J. Exp. Biol.* 208:2753–63
Standen EM, Lauder GV. 2007. Hydrodynamic function of dorsal and anal fins in brook trout (*Salvelinus fontinalis*). *J. Exp. Biol.* 210:325–39
Taft NK, Taft BN. 2012. Functional implications of morphological specializations among the pectoral fin rays of the benthic longhorn sculpin. *J. Exp. Biol.* 215:2703–10
Taguchi M, Liao JC. 2011. Rainbow trout consume less oxygen in turbulence: the energetics of swimming behaviors at different speeds. *J. Exp. Biol.* 214:1428–36
Tangorra JL, Gericke T, Lauder GV. 2011a. Learning from the fins of ray-finned fishes for the propulsors of unmanned undersea vehicles. *Mar. Technol. Soc. J.* 45:65–73
Tangorra JL, Lauder GV, Hunter I, Mittal R, Madden PG, Bozkurttas M. 2010. The effect of fin ray flexural rigidity on the propulsive forces generated by a biorobotic fish pectoral fin. *J. Exp. Biol.* 213:4043–54
Tangorra JL, Phelan C, Esposito C, Lauder GV. 2011b. Use of biorobotic models of highly deformable fins for studying the mechanics and control of fin forces in fishes. *Integr. Comp. Biol.* 51:176–89
Triantafyllou MS, Triantafyllou GS, Yue DKP. 2000. Hydrodynamics of fishlike swimming. *Annu. Rev. Fluid Mech.* 32:33–53
Tytell ED. 2004. Kinematics and hydrodynamics of linear acceleration in eels, *Anguilla rostrata*. *Proc. R. Soc. B* 271:2535–40
Tytell ED. 2006. Median fin function in bluegill sunfish *Lepomis macrochirus*: streamwise vortex structure during steady swimming. *J. Exp. Biol.* 209:1516–34
Tytell ED, Lauder GV. 2004. The hydrodynamics of eel swimming. I. Wake structure. *J. Exp. Biol.* 207:1825–41
Tytell ED, Lauder GV. 2008. Hydrodynamics of the escape response in bluegill sunfish, *Lepomis macrochirus*. *J. Exp. Biol.* 211:3359–69
Tytell ED, Standen EM, Lauder GV. 2008. Escaping Flatland: three-dimensional kinematics and hydrodynamics of median fins in fishes. *J. Exp. Biol.* 211:187–95
van Ginneken VJT, Antonissen E, Müller UK, Booms R, Eding E, et al. 2005. Eel migration to the Sargasso: remarkably high swimming efficiency and low energy costs. *J. Exp. Biol.* 208:1329–35
van Ginneken VJT, van den Thillart GEEJM. 2000. Eel fat stores are enough to reach the Sargasso. *Nature* 403:156–57
Videler JJ. 1993. *Fish Swimming*. New York: Chapman & Hall
Walker JA, Westneat MW. 1997. Labriform propulsion in fishes: kinematics of flapping aquatic flight in the bird wrasse *Gomphosus varius* (Labridae). *J. Exp. Biol.* 200:1549–69
Wardle CS, Videler JJ, Altringham JD. 1995. Tuning in to fish swimming waves: body form, swimming mode and muscle function. *J. Exp. Biol.* 198:1629–36
Webb PW. 1975. *Hydrodynamics and Energetics of Fish Propulsion*. Bull. Fish. Res. Board Can. 190. Ottawa, Can.: Dep. Environ. Fish. Mar. Serv.

Webb PW, Blake RW. 1985. Swimming. In *Functional Vertebrate Morphology*, ed. M Hildebrand, DM Bramble, KF Liem, DB Wake, pp. 110–28. Cambridge, MA: Harvard Univ. Press
Webb PW, Gerstner CL, Minton S. 1996. Station-holding by the mottled sculpin, *Cottus bairdi* (Teleostei: Cottidae), and other fishes. *Copeia* 1996:488–93
Webb PW, Keyes RS. 1982. Swimming kinematics of sharks. *Fish. Bull.* 80:803–12
Webb PW, Kostecki PT, Stevens ED. 1984. The effect of size and swimming speed on the locomotor kinematics of rainbow trout. *J. Exp. Biol.* 109:77–95
Webb PW, Weihs D, eds. 1983. *Fish Biomechanics*. New York: Praeger
Wen L, Lauder GV. 2013. Understanding undulatory locomotion in fishes using an inertia-compensated flapping foil robotic device. *Bioinspir. Biomim.* 8:046013
Wen L, Weaver JC, Lauder GV. 2014. Biomimetic shark skin: design, fabrication, and hydrodynamic function. *J. Exp. Biol.* 217:1656–66
Westneat MW. 1996. Functional morphology of aquatic flight in fishes: kinematics, electromyography, and mechanical modeling of labriform locomotion. *Am. Zool.* 36:582–98
Westneat MW, Hale ME, McHenry MJ, Long JH Jr. 1998. Mechanics of the fast-start: muscle function and the role of intramuscular pressure in the escape behavior of *Amia calva* and *Polypterus palmas*. *J. Exp. Biol.* 210:3041–55
Wilga C, Lauder GV. 2000. Three-dimensional kinematics and wake structure of the pectoral fins during locomotion in leopard sharks *Triakis semifasciata*. *J. Exp. Biol.* 203:2261–78
Wilga C, Lauder GV. 2001. Functional morphology of the pectoral fins in bamboo sharks, *Chiloscyllium plagiosum*: benthic versus pelagic station holding. *J. Morphol.* 249:195–209
Wilga C, Lauder GV. 2002. Function of the heterocercal tail in sharks: quantitative wake dynamics during steady horizontal swimming and vertical maneuvering. *J. Exp. Biol.* 205:2365–74
Wilga C, Maia A, Nauwelaerts S, Lauder GV. 2012. Prey handling using whole body fluid dynamics in batoids. *Zoology* 115:47–57
Williams R, Neubarth N, Hale ME. 2013. The function of fin rays as proprioceptive sensors in fish. *Nat. Commun.* 4:1729
Windsor SP, Norris SE, Cameron SM, Mallinson GD, Montgomery JC. 2010. The flow fields involved in hydrodynamic imaging by blind Mexican cave fish (*Astyanax fasciatus*). Part II: gliding parallel to a wall. *J. Exp. Biol.* 213:3832–42
Windsor SP, Tan D, Montgomery JC. 2008. Swimming kinematics and hydrodynamic imaging in the blind Mexican cave fish (*Astyanax fasciatus*). *J. Exp. Biol.* 211:2950–59
Wu G, Yang Y, Zeng L. 2007. Routine turning maneuvers of koi carp *Cyprinus carpio* koi: effects of turning rate on kinematics and hydrodynamics. *J. Exp. Biol.* 210:4379–89
Wu T, Brokaw CJ, Brennen C. 1975. *Swimming and Flying in Nature*. New York: Plenum
Xiong G, Lauder GV. 2014. Center of mass motion in swimming fish: effects of speed and locomotor mode during undulatory propulsion. *Zoology* 117:269–81
Youngerman ED, Flammang BE, Lauder GV. 2014. Locomotion of free-swimming ghost knifefish: anal fin kinematics during four behaviors. *Zoology* 117:337–48
Zhu D, Ortega CF, Motamedi R, Szewciw L, Vernerey F, Barthelat F. 2012. Structure and mechanical performance of a "modern" fish scale. *Adv. Eng. Mater.* 14:B185–94